ECHO-ENABLED HARMONIC GENERATION AT ELECTRON STORAGE RINGS*

S. Khan†, B. Büsing, C. Mai, A. Radha Krishnan, Z. Usfoor, V. Vijayan
Department of Physics and Center for Synchrotron Radiation (DELTA),
TU Dortmund University, Dortmund, Germany
W. Salah, Department of Physics, The Hashemite University, Zarqa, Jordan

Abstract

Echo-enabled harmonic generation (EEHG) has been proposed as a seeding method for free-electron lasers but can also be employed to generate ultrashort radiation pulses at electron storage rings. Due to the interaction of electrons with femtosecond laser pulses in two undulators (”modulators”), each followed by a magnetic chicane, a longitudinal phase space structure with high harmonic content is produced, which gives rise to coherent emission of radiation at harmonics of the laser wavelength. The length of the coherently emitted pulses in a third undulator (”radiator”) is given by the laser pulse duration. Thus, EEHG pulses can be three orders of magnitude shorter but still more intense than conventional synchrotron light pulses. The latest results of the worldwide first EEHG demonstration experiment at a storage ring (DELTA at the TU Dortmund University) are presented.

INTRODUCTION

Electron storage rings producing synchrotron radiation (SR) in the ultraviolet to X-ray range are standard tools in physics, materials research, chemistry, and biology to study the structure of matter on the atomic scale [1]. Significant progress has recently been made in reducing the beam emittance. The pulse duration, however, is still several tens of picoseconds, while dynamical changes of atoms and molecules such as phase transitions, chemical reactions, lattice vibrations etc. are on the sub-picosecond scale. Femtosecond time resolution at small wavelengths is obtained by laser-based plasma sources and high-harmonic generation, and more recently by high-gain free-electron lasers (FELs) [2]. While around 10 FELs worldwide serve one user at a time with the bunch rate of a linear accelerator, there are about 50 SR sources [3] supplying multiple beamlines simultaneously with stable and tunable radiation at a rate of up to 500 MHz. It is therefore worthwhile to consider methods to improve the time resolution for experiments at storage rings.

Instead of shortening the electron bunches in SR facilities, a pulse duration below 100 fs may be obtained from a ”slice” within a long bunch interacting with a femtosecond laser pulse in an undulator (”modulator”) and causing a periodic modulation of the electron energy. When off-energy electrons are transversely displaced by dispersion, their SR from a second undulator (”radiator”) can be extracted using an aperture [4–6]. The ratio of electrons in the slice and the bunch is $\approx 10^{-3}$, and the fraction of incoherent SR in the short pulse is even lower.

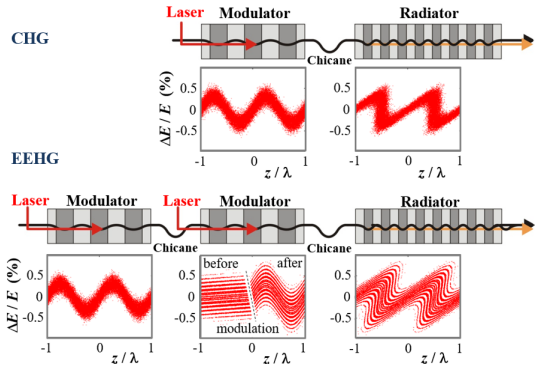

Figure 1: Layout of the CHG and EEHG setup and respective distributions of electrons in phase space (relative energy offset $\Delta E/E$ versus longitudinal position z in units of λ_L).

Coherent emission at harmonics of the laser wavelength λ_L is obtained when the laser-induced energy modulation is converted to a periodic density pattern by a dispersive section (”chicane”). The SR intensity from the short slice is then proportional to the square of the number of electrons and the squared bunching factor b_h^2. Thus, radiation at a laser harmonic h (wavelength λ_L/h) can exceed the incoherently emitted radiation from the whole bunch by an order of magnitude or more. In this scheme, known as coherent harmonic generation (CHG, Fig. 1, top) [7], the storage ring equivalent to high-gain harmonic generation (HGHG) in seeded FELs [8], the bunching factor decreases as $b_h \sim \exp(-h^2)$.

Echo-enabled harmonic generation (EEHG, Fig. 1, bottom) was proposed as an FEL seeding scheme to reach higher harmonics [9]. Here, a twofold laser-electron interaction leads to a more complex density modulation with the bunching factor decreasing as $b_h \sim h^{-1/3}$. EEHG was demonstrated at linear accelerators [10–13] and was implemented for user operation at FERMI (Trieste, Italy) [14].

For short-pulse generation at SR sources, different EEHG setups were proposed with all undulators and chicanes in one long [15] or in two consecutive straight sections [16–18], or even using the whole storage ring as a chicane [19]. As a worldwide first implementation at a storage ring, a demonstration experiment was realized in a single 5 m long straight section of the 1.5-GeV SR source DELTA [20] operated by the TU Dortmund University in Germany.

* Work supported by DFG (contract INST212/236-1), BMBF (contracts 05K22PE1 and 05K22PE4), and by the Federal State NRW.
† shaukat.khan@tu-dortmund.de

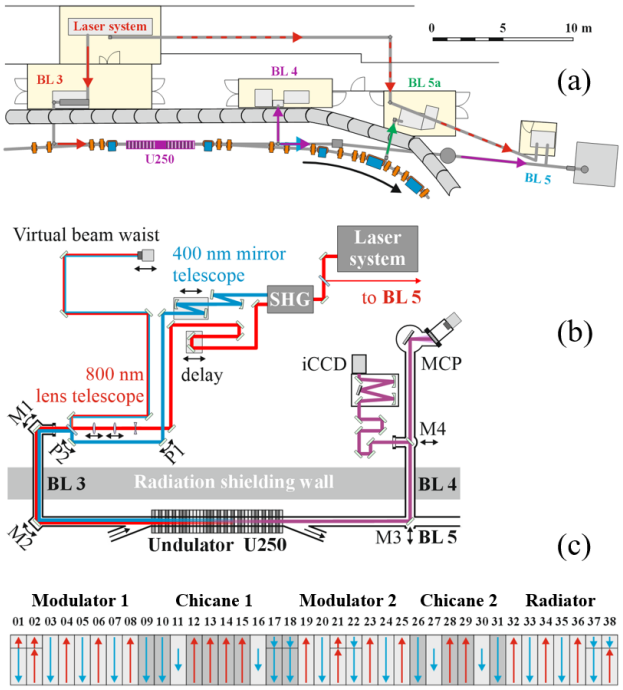

Figure 2: (a) DELTA short-pulse facility comprising a laser system, a beamline (BL 3) directing seed pulses to the undulator U250, a diagnostics beamline (BL 4), a soft-X-ray user beamline (BL 5), and a THz beamline (BL 5a). (b) Path of 800-nm (red) and 400-nm (blue) laser beams after second-harmonic generation (SHG). EEHG radiation from the U250 radiator is directed to two alternative spectrometers. (c) Magnetic field configuration (red and blue arrows) of the electromagnetic undulator U250 with 38 poles.

EXPERIMENTAL SETUP

The DELTA short-pulse facility based on CHG was implemented in 2011 using the electromagnetic undulator U250 in an optical-klystron configuration (modulator, chicane, radiator) [15].

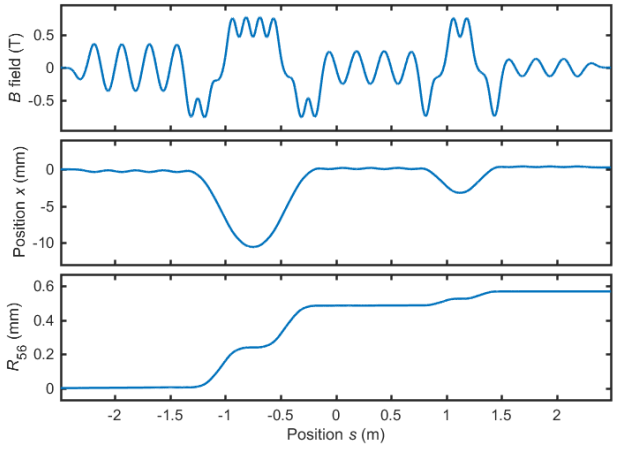

Figure 3: Vertical magnetic field (top), horizontal beam trajectory (center), and integrated longitudinal dispersion R_{56} (bottom) along the undulator U250.

Table 1: Parameters of the EEHG setup at DELTA

Parameter	Value
Storage ring circumference	115.2 m
Electron beam energy	1.5 GeV
Max. single-/multibunch current	20/140 mA
Horizontal emittance	16 nm rad
Relative energy spread	$8 \cdot 10^{-4}$
Bunch length (FWHM)	85 ps
Laser pulse energy (800 nm)	8.0 mJ
Pulse energy after SHG (400/800 nm)	2.4/2.4 mJ
Laser pulse repetition rate	1 kHz
Min. laser pulse duration (FWHM)	40 fs
U250 undulator period	0.25 m
U250 total length	4.75 m
U250 max. K parameter	10.4
Periods per EEHG undulator	4
Max. R_{56} of first/second chicane	550/105 µm

Figure 2 shows the general layout (a), the laser concept (b), and the undulator U250 (c) rewired in 2022 to implement the EEHG configuration (modulator, chicane, modulator, chicane, radiator) [21, 22]. Boards with copper bars allow to switch from this setup to a standard undulator. Split coils at poles 01, 02, 17, 18, 21, 22, 37, and 38 allow to yield 1/4, 3/4, 1/2, or 1/1 of the full magnetic field by powering only one partial coil or both in opposite or parallel direction. In poles 11, 16, 27, and 30, the required lower field is obtained by dedicated power supplies. These are undulator endpoles interleaved with chicanes, and setting two consecutive undulators to different wavelength causes a nonzero R_{52} component leading to a longitudinal smearing $\sigma_z = R_{52} \cdot \sigma_{x'}$ depending on the angular spread $\sigma_{x'}$. However, a corrector current with opposite sign applied to the two endpoles within a chicane allows to minimize the R_{52} value [23, 24], and fine-tuning of these currents mitigates non-closure of the chicanes due to magnetic saturation [25]. In total, 14 power supplies are in use providing a maximum current of 400 A for the undulators and 800 A for the chicanes. The maximum K value of each undulator is 10.4, corresponding to a wavelength of 800 nm at 1.5 GeV.

Table 1 summarizes the relevant parameters of the storage ring, the laser system, and the undulator U250. Figure 3 shows the vertical magnetic field, horizontal beam trajectory, and integrated longitudinal dispersion R_{56}. In this example, the three undulators are tuned to 800 nm, 400 nm, and 133 nm, respectively.

The two seed pulses required for EEHG are generated from a single Ti:sapphire laser system [26]. Pulses with wavelength 800 nm pass a nonlinear crystal (BBO) to generate the second harmonic, which is focused into the second modulator using two curved mirrors. The residual 800-nm radiation is focused by three lenses into the first modulator.

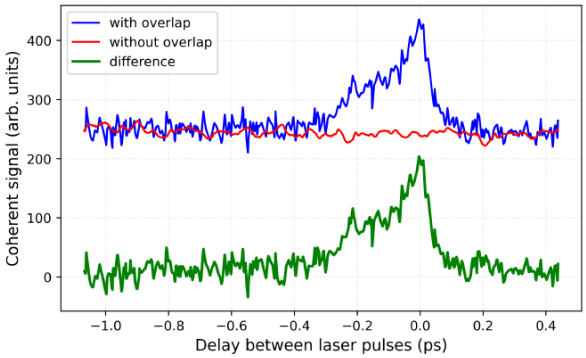

Figure 4: Radiation intensity at wavelength 114 nm as function of the delay between two seed laser pulses. Blue: Raw signal. Red: Signal with longitudinally displaced laser pulses. Green: Difference between blue and red curve.

RESULTS

A photodiode and a streak camera [27] are used for the longitudinal alignment of the laser pulses with a single bunch. Coherently emitted THz and sub-THz radiation from energy-modulated electrons leaving a dip in the longitudinal bunch profile provides a reliable signature for laser-induced energy modulation [28, 29]. The transverse alignment is first optimized for 800-nm pulses by maximizing the THz signal with the motorized mirrors M1 and M2 (Fig. 2). After optimizing the alignment of 400-nm pulses using the same mirrors, the piezo-driven mirrors P1 and P2 are iteratively tuned to recover the previous M1 and M2 settings while maintaining the THz signal. When scanning the relative timing of the two laser pulses, their overlap is found by observing interference fringes in the THz intensity. The largest fringe exhibits a narrow dip when both pulses interact with the same electrons, thus reducing the number of coherently emitting electrons [22]. Radiation at and above 200 nm is observed by a Czerny-Turner spectrometer equipped with a gated iCCD camera [30] at beamline BL 4. For EEHG radiation below 200 nm, an in-vacuum grating spectrometer with a gated microchannel plate (MCP) [31] is employed.

After first results with radiation at 267 nm [22], the project was plagued by technical problems. EEHG signals at wavelengths 160 nm and 114 nm ($h = 5$ and 7) were obtained in 2024 [23, 24]. With further improvements, EEHG signals down to 73 nm ($h = 11$) were observed [25]. An example of a scan of the relative laser timing is shown in Fig. 4 for 114 nm. The asymmetric shape of the EEHG signal may be due to an afterpulse caused by third-order dispersion.

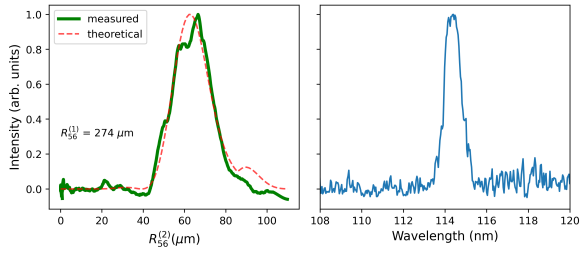

Figure 5: Left: Background-subtracted and normalized intensity (green line) and theoretical expectation (red dashed line) as function of the longitudinal dispersion $R_{56}^{(2)}$ of the second chicane for $R_{56}^{(1)} = 274\,\mu m$ of the first chicane. Right: Spectral distribution at $R_{56}^{(2)} = 65\,\mu m$.

The occurrence of EEHG radiation depends on the longitudinal dispersion of both chicanes. Experimentally, it is easier to scan the $R_{56}^{(2)}$ value of the second chicane while keeping the first chicane constant, because changing $R_{56}^{(1)}$ would shift the electron arrival time at the second modulator. The $R_{56}^{(2)}$ scan in Fig. 5 (left) demonstrates that the observed radiation intensity (green line) changes as expected by theory (red dashed line) according to Ref. 9. Similar results are obtained for all odd harmonics from $h = 5$ to 11 assuming a relative energy modulation amplitude of $\Delta E/E = 0.12$ after the first modulator and 0.14 after the second. Within these harmonics, the ratio of coherent signal and incoherent background reduces from 5.3 to 1.4, which differs from analytical estimates but is consistent with simulation results taking realistic magnetic fields and a 3-dimensional laser beam waist into account [25]. With (1.0 ± 0.1) nm (FWHM), the measured bandwidth (right part of Fig. 5) is much smaller than the spectral width of incoherently emitted radiation from an undulator with only 4 periods. Considering the time-bandwidth product for a Gaussian pulse, the corresponding pulse duration is ≥ 19 fs (FWHM).

OUTLOOK

The present setup with only 4 periods per undulator, moderate longitudinal dispersion, and limited laser power is not ideally suited for EEHG. Nevertheless, studying these limitations and gaining operational experience yields valuable information in view of future EEHG implementations at storage rings. The relative energy modulation amplitude and longitudinal dispersion can be further improved by reducing the beam energy at the expense of beam lifetime. Low-energy operation has been tested down to 0.8 GeV [32].

Contrary to other proposed EEHG setups, the present magnetic configuration has a total length of only 4.75 m and fits in a typical straight section of an SR source. For an equally short setup, permanent-magnet undulators with shorter and more periods can greatly improve the energy modulation and the radiation output. Together with a laser upgrade, a user-compatible facility would be within reach [24, 25]. A storage ring with shorter bunches (higher radiofrequency voltage and/or lower momentum compaction factor) yields a better signal-to-background ratio, since the fraction of energy-modulated electrons is larger. Lower beam emittance and energy spread would further improve the signal. As another option, seeding with shorter wavelengths would reduce the required modulator period length and could be another step to reach shorter EEHG wavelengths.

ACKNOWLEDGEMENTS

The continuous support of the whole DELTA team is gratefully acknowledged.

REFERENCES

[1] E. Jaeschke, S. Khan, J. R. Schneider, and J. B. Hastings (Eds.), *Synchrotron Light Sources and Free-Electron Lasers*, Cham, Switzerland: Springer, 2020. doi:10.1007/978-3-030-23201-6

[2] R. Schoenlein *et al.*, "Recent advances in ultrafast X-ray sources", *Phil. Trans. R. Soc.*, vol. A 377, p. 20180384, 2019. doi:10.1098/rsta.2018.0384

[3] https://lightsources.org/

[4] A. A. Zholents and M. S. Zolotorev, "Femtosecond X-ray pulses of synchrotron radiation", *Phys. Rev. Lett.*, vol. 76, pp. 912-915, 1996. doi:10.1103/PhysRevLett.76.912

[5] R. W. Schoenlein *et al.*, "Generation of Femtosecond Pulses of Synchrotron Radiation", *Science*, vol. 287, pp. 2237-2240, 2000. doi:10.1126/science.287.5461.2237

[6] S. Khan *et al.*, "Femtosecond undulator radiation from sliced electron bunches", *Phys. Rev. Lett.*, vol. 97, p. 074801, 2006. doi:10.1103/PhysRevLett.97.074801

[7] B. Girard *et al.*, "Optical frequency multiplication by an optical klystron", *Phys. Rev. Lett.*, vol. 53, pp. 2405-2409, 1984. doi:10.1103/PhysRevLett.53.2405

[8] L. H. Yu, "Generation of intense uv radiation by subharmonically seeded single-pass free-electron lasers", *Phys. Rev. A*, vol. 44, pp. 5178-5193, 1991. doi:10.1103/PhysRevA.44.5178

[9] D. Xiang and G. Stupakov, "Echo-enabled harmonic generation free electron laser", *Phys. Rev. Accel. Beams*, vol. 12, p. 030702, 2009. doi:10.1103/PhysRevSTAB.12.030702

[10] D. Xiang *et al.*, "Demonstration of the echo-enabled harmonic generation technique for short-wavelength seeded free electron lasers", *Phys. Rev. Lett.*, vol. 105, p. 114801, 2010. doi:10.1103/PhysRevLett.105.114801

[11] Z. T. Zhao *et al.*, "First lasing of an echo-enabled harmonic generation free-electron laser", *Nat. Photonics*, vol. 6, pp. 360-363, 2012. doi:10.1038/nphoton.2012.105

[12] E. Hemsing *et al.*, "Echo-enabled harmonics up to the 75th order from precisely tailored electron beams", *Nat. Photonics*, vol. 10, pp. 512-515, 2016. doi:10.1038/nphoton.2016.101

[13] P. R. Ribič *et al.*, "Coherent soft X-ray pulses from an echo-enabled harmonic generation free-electron laser", *Nat. Photonics*, vol. 13, pp. 555-561, 2019. doi:10.1038/s41566-019-0427-1

[14] C. Spezzani *et al.*, "Echo-enabled harmonic generation at FERMI FEL-1: Commissioning and initial user experience", in *Proc. 15th Int. Particle Accelerator Conf. (IPAC'24)*, Nashville, TN, USA, May 2024, pp. 1889-1892. doi:10.18429/JACoW-IPAC2024-WEAD3

[15] S. Khan *et al.*, "Coherent harmonic generation at DELTA: a new facility for ultrashort pulses in the VUV and THz regime", *Synchrotron Radiat. News*, vol. 24:5, pp. 18-23, 2011. doi:10.1080/08940886.2011.618092

[16] C. Evain *et al.*, "Soft x-ray femtosecond coherent undulator radiation in a storage ring", *New J. Phys.*, vol. 14, p. 023003, 2012. doi:10.1088/1367-2630/14/2/023003

[17] J.-G. Hwang *et al.*, "Generation of intense and coherent sub-femtosecond X-ray pulses in electron storage rings", *Sci. Reports*, vol. 10, p. 10093, 2020. doi:10.1038/s41598-020-67027-0

[18] X. Yang *et al.*, "Optimization of echo-enabled harmonic generation toward coherent EUV and soft X-ray free-electron laser at NSLS-II", *Sci. Reports*, vol. 12, p. 9437, 2022. doi:10.1038/s41598-022-13702-3

[19] H. T. Li, W. W. Gao, Q. K. Jia ,and L. Wang, "Echo-enabled harmonic generation based on Hefei storage ring", in *Proc. 4th Int. Particle Accelerator Conf. (IPAC'13)*, Shanghai, China, May 2013, pp. 1208-1210.

[20] M. Tolan, T. Weis, C. Westphal, and K. Wille, "DELTA: Synchrotron light in Nordrhein-Westfalen", *Synchrotron Radiat. News*, vol. 16, no. 2, pp. 9-11, 2003. doi:10.1080/08940880308603005

[21] B. Büsing *et al.*, "Preparatory experimental investigations in view of EEHG at the DELTA storage ring", in *Proc. 40th Free-Electron Laser Conf. (FEL'22)*, Trieste, Italy, August 2022, pp. 313-316. doi:10.18429/JACoW-FEL2022-TUP70

[22] S. Khan *et al.*, "SPEED: Worldwide first EEHG implementation at a storage ring", in *Proc. 14th Int. Particle Accelerator Conf. (IPAC'23)*, Venice, Italy, May 2023, pp. 1057-1060. doi:10.18429/JACoW-IPAC2023-MOPM032

[23] S. Khan *et al.*, "Commissioning of echo-enabled harmonic generation at the DELTA storage ring", in *Proc. 41th Free-Electron Laser Conf. (IPAC'24)*, Warsaw, Poland, August 2024, MOAI02.

[24] S. Khan *et al.*, "Echo-enabled harmonic generation at the DELTA storage ring", in *Proc. 16th Int. Particle Accelerator Conf. (IPAC'25)*, Taipei, Taiwan, June 2025, pp. 87-90. doi:10.18429/JACoW-IPAC2025-MOPB007

[25] A. Radha Krishnan, *First Demonstration of Echo-Enabled Harmonic Generation in a Storage Ring and Deep Learning for Beam Diagnostics*, Dissertation, TU Dortmund University, 2026. doi:10.17877/DE290R-26603

[26] Coherent Legend Elite Duo, https://www.coherent.com/

[27] Optronix Optoscope, https://optronis.com/

[28] P. Ungelenk *et al.*, "Studies of ultrashort THz pulses at DELTA", in *Proc. 5th Int. Particle Accelerator Conf. (IPAC'14)*, Dresden, Germany May 2014, pp. 1936-1939. doi:10.18429/JACoW-IPAC2014-WEPRO002

[29] C. Mai *et al.*, "Observation of coherent pulses in the sub-THz range at DELTA", in *Proc. 6th Int. Particle Accelerator Conf. (IPAC'15)*, Richmond, VA, USA, May 2015, pp. 823-826. doi:10.18429/JACoW-IPAC2015-MOPHA023

[30] Oxford Instruments, Andor iStar 334T, https://andor.oxinst.com

[31] HP Spectroscopy easyLight XUV, https://www.hp-spectroscopy.com

[32] C. Mai *et al.*, "Observation of coherent terahertz bursts during low-energy operation of DELTA", in *Proc. 14th Int. Particle Accelerator Conf. (IPAC'23)*, Venice, Italy, May 2023, pp. 1061-1063. doi:10.18429/JACoW-IPAC2023-MOPM033